

11-18-2008

Recent Extreme Avalanches: Triggered by Climate Change?

Christian Huggel

Jacqueline Caplan-Auerbach

Western Washington University, jackie.caplan-auerbach@wwu.edu

Rick Wessels

Follow this and additional works at: https://cedar.wwu.edu/geology_facpubs

 Part of the [Geology Commons](#), and the [Geophysics and Seismology Commons](#)

Recommended Citation

Huggel, Christian; Caplan-Auerbach, Jacqueline; and Wessels, Rick, "Recent Extreme Avalanches: Triggered by Climate Change?" (2008). *Geology Faculty Publications*. 45.
https://cedar.wwu.edu/geology_facpubs/45

This Article is brought to you for free and open access by the Geology at Western CEDAR. It has been accepted for inclusion in Geology Faculty Publications by an authorized administrator of Western CEDAR. For more information, please contact westerncedar@wwu.edu.

Recent Extreme Avalanches: Triggered by Climate Change?

PAGES 469–470

On 25 September 2008, seismometers operated by the Alaska Volcano Observatory (AVO) registered strong ground shaking. On the basis of previous experience with such large seismic signals, AVO personnel were able to rapidly identify the seismic event as an avalanche. Two days later, an AVO overflight of Iliamna volcano, near Alaska's Cook Inlet, confirmed that a massive chunk of glacial ice and rock had broken free from its position on the upper flanks of the volcano, generating a massive avalanche that could have buried an entire town had it occurred in a more populated area.

Rapidly moving rock, ice, or debris avalanches, such as the one that occurred on Iliamna, can be highly destructive and deadly. Similar events have caused the deaths of hundreds to thousands of people [Keefe and Larsen, 2007]. In general, avalanches that move more than 1 million cubic meters of material are rare. However, a remarkable series of large avalanches recently occurred in Alaska and the Caucasus, providing a new opportunity to better understand this type of hazard. All events initiated in steep mountain slopes, involved rock and significant amounts of ice, and traveled for 10–35 kilometers.

Combined geophysical methods can be applied to investigate the failure and propagation of large avalanches. We primarily use seismic signals, coupled with ground-based and remote temperature data. In temperature-sensitive glacier and permafrost environments, thermal perturbations are highly relevant because changes from frozen to liquid water can fundamentally affect slope stability. In the cases presented here, geophysical methods support the analysis of possible thermal perturbations due to volcanic activity and climate change. Improved detection and analysis methods are particularly important in the context of ongoing and likely accelerating climate change, where related hazards are becoming increasingly problematic.

Recent Extreme Avalanches

Three recent groups of avalanches were large scale, well documented, and in most cases, seismically detected. In the case of avalanches on Iliamna volcano and Mount Steller, Alaska, the events were chosen for study because of the availability of seismic and thermal data. Study of the 2002 failure of the Kolka glacier in the Caucasus was motivated by the size and deadly nature of the avalanche.

The September 2008 avalanche described above is just one of a number of similar events that have taken place on Iliamna volcano (elevation 3050 meters). These events typically released between 10 and 30 million cubic meters of material [Caplan-Auerbach and Huggel, 2007]. Using historical aerial photographs and satellite images, we were able to document avalanches since 1960. In the past 15 years, the frequency of avalanches has increased from one reported every decade to approximately one reported every 3–5 years [Huggel et al., 2007]. This may reflect enhanced monitoring of the volcano, or changes in trigger mechanisms.

Alaskan activity of large avalanches is not confined to Iliamna, however. On 14 September 2005, a summit glacier on the steep south face of Mount Steller (elevation 3230 meters),

in Alaska's Chugach Mountains, failed as a major avalanche of rock and ice (Figure 1). The avalanche, which released and entrained about 50 million cubic meters of debris, traveled 9 kilometers and eventually stopped on Bering glacier. The event was recorded worldwide on seismometers [Huggel et al., 2008].

The largest ice-rock avalanche on record occurred in 2002 in Russia's Kazbek region of the northern Caucasus Mountains. On the northeastern face of Dzhimari-khokh (elevation 4780 meters), 10–20 million cubic meters of rock and glacier ice failed and fell onto Kolka glacier [Kääb et al., 2003]. Because of the high-energy impact and probably unstable glacier conditions, the Kolka glacier was almost completely swept up by the avalanche. At speeds of up to 80 meters per second, a mass of more than 100 million cubic meters of ice, rock, and debris rushed down the valley and formed a major ice dam in front of a gorge. The liquid parts of the avalanche traveled farther downstream as a devastating debris flow, killing more than 100 people. We used high-resolution satellite images and data from extensive glaciological and geomorphological field studies to assess postdisaster hazards to gain a better understanding of complex avalanche processes.

Seismic Signals From Avalanches

Seismic records were crucial for the detection and analysis of these avalanches. Because they occurred in remote regions, the avalanches were first identified in

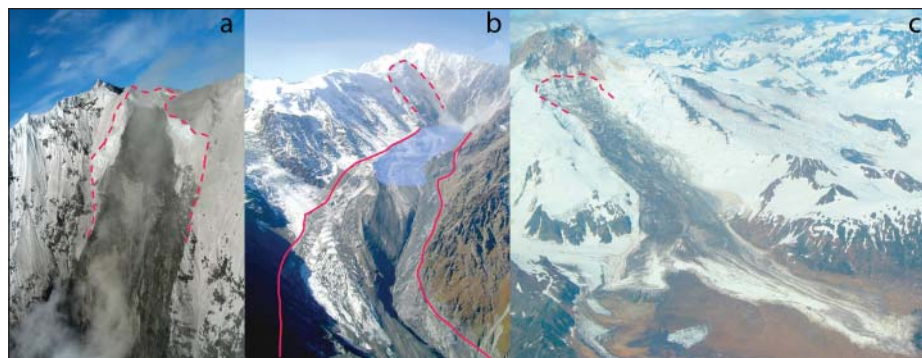


Fig. 1. Recent extreme ice-rock avalanches. (a) Mount Steller, Alaska, a few hours after the avalanche in 2005. The failure zone is indicated by the dashed line. (b) The upper part of the Kolka avalanche path. Initial slope failure (dashed line), the former location of the impacted Kolka glacier (transparent blue), and avalanche path (solid line) are indicated. (c) An avalanche on Iliamna volcano in July 2003. The distance traveled by the avalanche was about 8.5 kilometers. Photos by R. Homburger, I. Galushkin, and R. Wessels, respectively.

seismic data. On the basis of the duration of the seismic record and the distance traveled, we reconstructed average avalanche speeds of 100 meters per second for the Mount Steller event, 20–75 meters per second for the seven Iliamna avalanches, and 50–80 meters per second for the Kolka avalanche.

The seismograms have a spindle-shaped form typical of mass movements [Norris, 1994]. A more detailed analysis of the seismic signals, however, reveals that the Mount Steller and Iliamna avalanches exhibited a sequence of small ($M < 1$) precursory earthquakes that have not been observed prior to other slope failures (Figure 2). These signals start between one half and 2 hours before the avalanche and have thus far been observed only in failures in ice.

The precursory portion of the avalanche seismicity follows a predictable pattern of discrete earthquakes that gradually evolve into a continuous ground shaking. Each sequence culminates in a strong broadband spindle-shaped signal (Figure 2). These precursory signals have been interpreted as deformation and slip at the glacier base that increase as failure approaches [Caplan-Auerbach and Huggel, 2007]. A similar analysis could not be performed for the Kolka avalanche, as the nearest digital seismic station was too far away to record any precursory activity.

Examining Avalanche Triggers With Multisource Temperature Data

To further investigate how these events could be related to thermal perturbations, we explored different methods of ground, surface, and air temperature data.

The Advanced Spaceborne Thermal Emission and Reflection Radiometer (ASTER) satellite provides an excellent opportunity to collect thermal data with high spatial and spectral resolution (ground resolution of 90 meters in five spectral thermal infrared channels [see Pieri and Abrams [2004]]. For Iliamna, a subpixel heat source calculation based on ASTER data indicated a number of hot spots near the avalanche initiation zone with temperatures of 30° to more than 300°C, probably related to fumarolic activity [Huggel et al., 2007]. Melting of glacier ice due to volcanic heat sources is likely to reduce the strength at the base of the glacier and promote failure.

In the absence of direct field measurements at Iliamna, glacier mass balance modeling combined with aggregated climate data and satellite observations suggests that (1) the observed surface melting in the avalanche initiation zone is driven primarily by volcanic heat flux, and (2) snow accumulation rates in the initiation zone are about 10 meters of snow per year. Such continuously high precipitation implies frequent recharging of the avalanche reservoirs. Preliminary conclusions thus point to both a climatic and volcanic control on avalanche formation on Iliamna. For more on avalanches at Iliamna, see the electronic supplement to this *Eos* issue (http://www.agu.org/eos_elec/).

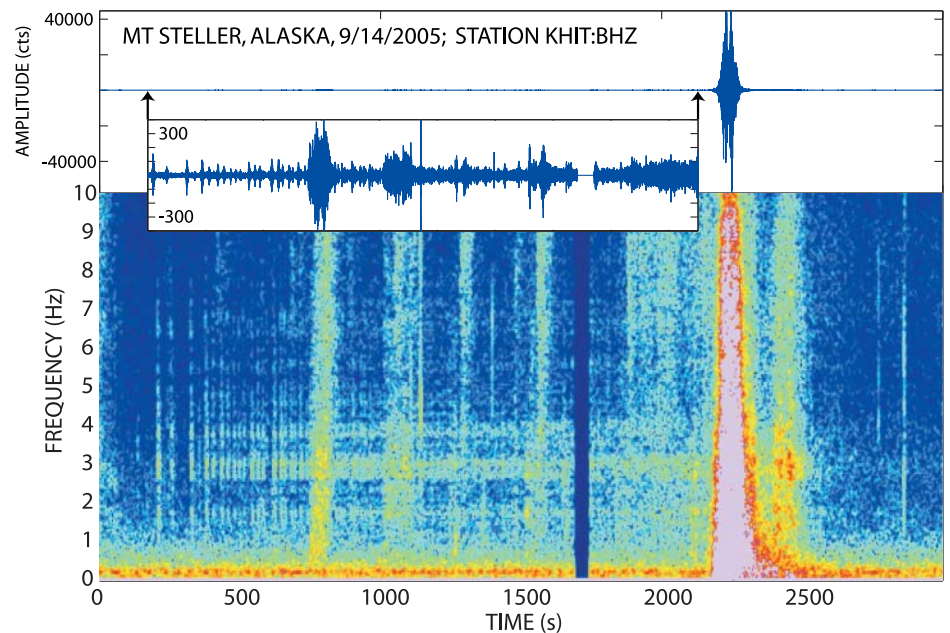


Fig. 2. Seismic signals associated with the 2005 avalanche at Mount Steller. A time series (top) and a spectrogram (bottom) show ground shaking associated with the Mount Steller event, as recorded at a seismometer 12 kilometers southwest of Mount Steller. Warmer colors in the spectrogram represent stronger amplitudes. Precursory seismicity interpreted as glacier slip events is visible as a sequence of discrete events between 200 and 2000 seconds, at specific frequencies of 1–7 hertz, while small precursory avalanches can be recognized at roughly 750, 1000, 1200, and 1500 seconds with a broadband spectrum. The avalanche is visible at approximately 2150 seconds into the record.

Atmospheric warming in recent decades has been particularly strong in Alaska (0.03°–0.05°C per year [Symon et al., 2005]). To investigate a possible influence of rising temperatures on slope stability in glacier and permafrost environments, we analyzed the existing record of troposphere temperatures for Mount Steller derived from the closest radiosonde data (Yakutat, 270 kilometers southeast of Mount Steller; Figure 3).

The decadal warming trend of 0.3°–0.4°C for the past 15 years at the level of Mount Steller's summit is consistent with the general warming pattern in Alaska. The mean annual air temperature observed at the summit is –10°C. However, unusually warm summer temperatures in 2004–2005, far above freezing, have been observed in the troposphere temperature data (Figure 3). General warming, along with daily and seasonal variations in temperature, can produce melting conditions at the glacier surface that can be accompanied by infiltration and latent heat dissipation processes that can amplify the ice's warming trend. Both decadal and seasonal warming have likely produced melting of ice and possibly permafrost degradation that could have contributed to the 2005 avalanche.

In the Caucasus, a number of temperature loggers were installed in steep rock walls near the avalanche failure area at approximately 10 centimeters below the surface. Temperatures measured over more than 1 year clearly indicated permafrost in the area that failed, with possible thawing in the lower section of the failure area. How permafrost degradation affects slope stability in

steep terrain is not yet well understood, but theoretical considerations suggest that the transition from frozen to unfrozen rock can have a critical effect on slope stability [Gruber and Haeblerli, 2007].

Assessing Hazards in a Changing World

In view of the potential effects of climate change on avalanche and landslide hazards as well as the ongoing economic development of mountain regions coupled with population growth, it is crucial to monitor critical avalanche locations and establish readily available methods for early avalanche prediction.

The type of multisource thermal monitoring we present here is applicable even for regions with difficult access and poor field data. Seismic measurements can help constrain avalanche mechanisms, and precursory signals could one day facilitate early warning, assuming that those signals are timely and may be unambiguously identified in real time. An improved coupling of the presented methods to subsurface thermal modeling, numerical slope stability, and dynamic avalanche modeling is an additional critical goal. A number of research projects are currently investigating this coupling, with the hope that new insights from geophysical techniques will be helpful to hazard mitigation.

Acknowledgments

The studies were partly supported by the Swiss National Science Foundation, the Swiss

Agency for Development and Cooperation, and the USGS Mendenhall Postdoctoral Program. We acknowledge the Alaska Earthquake Information Center and the U.S./Japan ASTER science team for providing data; R. McGimsey, R. Homberger, and I. Galushkin for the photos; and H. Machguth for collaboration on glacier mass balance.

References

- Caplan-Auerbach, J., and C. Huggel (2007), Precursory seismicity associated with frequent, large avalanches on Iliamna volcano, Alaska, *J. Glaciol.*, 53(180), 128–140.
- Gruber, S., and W. Haerberli (2007), Permafrost in steep bedrock slopes and its temperature-related destabilization following climate change, *J. Geophys. Res.*, 112, F02S18, doi:10.1029/2006JF000547.
- Huggel, C., J. Caplan-Auerbach, C. F. Waythomas, and R. L. Wessels (2007), Monitoring and modeling ice-rock avalanches from ice-capped volcanoes: A case study of frequent large avalanches on Iliamna volcano, Alaska, *J. Volcanol. Geotherm. Res.*, 168, 114–136.
- Huggel, C., J. Caplan-Auerbach, S. Gruber, B. Molnia, and R. Wessels (2008), The 2005 Mt. Steller, Alaska, rock-ice avalanche: A large slope failure in cold permafrost, in *Proceedings of the Ninth International Conference on Permafrost*, vol. 1., pp. 747–752, Univ. of Alaska Fairbanks.
- Kääb, A., R. Wessels, W. Haerberli, C. Huggel, J. S. Kargel, and S. J. S. Khalsa (2003), Rapid ASTER imaging facilitates timely assessment of glacier hazards and disasters, *Eos Trans. AGU*, 84(13), 117, 121.
- Keefer, D. K., and M. C. Larsen (2007), Assessing landslide hazards, *Science*, 316(5828), 1136–1138.
- Norris, R. D. (1994), Seismicity of rockfalls and avalanches at three Cascade Range volcanoes: Implications for seismic detection of hazardous mass movements, *Bull. Seismol. Soc. Am.*, 84, 1925–1939.
- Pieri, D., and M. Abrams (2004), ASTER watches the world's volcanoes: A new paradigm for volcanological observations from orbit, *J. Volcanol. Geotherm. Res.*, 135, 13–28.
- Symon, C., L. Arris, and B. Heal (Eds.) (2005), *Arctic Climate Impact Assessment: Scientific Report*, 1042 pp., Cambridge Univ. Press, New York.

Author Information

Christian Huggel, Department of Geography, University of Zurich, Zurich, Switzerland; E-mail: christian.huggel@geo.uzh.ch; Jacqueline Caplan-Auerbach, Geology Department, Western Washington University, Bellingham; and Rick Wessels, Alaska Science Center, Alaska Volcano Observatory, U.S. Geological Survey, Anchorage

Mexican Forest Inventory Expands Continental Carbon Monitoring

PAGES 470–471

The terrestrial ecosystems of the North American continent represent a large reservoir of carbon and a potential sink within the global carbon cycle. The recent State of the Carbon Cycle Report [U.S. Climate Change Science Program (CCSP), 2007] identified the critical role these systems may play in mitigating effects of greenhouse gases emitted from fossil fuel combustion. However, there are currently large uncertainties in continental carbon models, and the scientific community's understanding of relevant carbon sources and sinks has been much less complete in Mexico than in Canada and the United States [Birdsey *et al.*, 2007].

One reason for this disparity has been a lack of systematic field data from throughout Mexico. Recently, though, new field and satellite inventory information has become available through two Mexican resource agencies, the Comisión Nacional Forestal (CONAFOR) and the Instituto Nacional de Estadística y Geografía (INEGI). This information has the potential to support new types of analysis within Mexico and to significantly augment efforts to characterize carbon dynamics at the continental scale. Moreover, because many of the forest types and land use issues present in Mexico can be found throughout Latin America, Mexico's support of carbon monitoring may provide a relevant example as other countries within the region develop their own inventories.

Improved Identification of Land Use Change

Much of the previous work [e.g., De Jong *et al.*, 2000; Maser *et al.*, 1997; Ordóñez *et al.*, 2006] done to quantify Mexican terrestrial carbon dynamics has focused on changes in carbon storage associated with land use change. National maps of land use produced by INEGI and other sources

covering different time periods over the past two to three decades have been a primary source of information in these efforts.

INEGI will continue to support land use change monitoring by releasing updated 1:250,000 maps of vegetation and land use in 2010. A recent addition to the process of updating these national maps is carried out by CONAFOR; consecutive satellite images are used to detect and map deforestation. A combination of imagery from the Moderate Resolution Imaging Spectroradiometer (MODIS), Landsat, and Satellite Pour l'Observation de la Terre (SPOT) platforms is used to identify hot spots of deforestation and digitize specific areas of change within these hot spots. Further satellite-based information about land use and land cover change is becoming available via Mexico's collaboration with both the North American Carbon Program's North American Forest Dynamics project [Goward *et al.*, 2008] and the North American Land Change Monitoring System conducted by the Commission for Environmental Cooperation (<http://www.cec.org>).

New National Vegetation Inventory Information

In addition to INEGI's maps of vegetation and land use, extensive field inventory data are now available from throughout Mexico. The National Forest and Soil Inventory (Inventario Nacional Forestal y de Suelos, or INFyS), initiated by CONAFOR in 2002, represents the first nationally consistent sample of Mexico's many diverse vegetation communities. More than 24,000 standardized forest inventory plots have been surveyed in a network that provides substantially improved monitoring across all of the country's vegetation types (Figure 1). The distribution of plots (using a 5 × 5 kilometer systematic sampling grid for temperate and high tropical forests, a 10 × 10 kilometer grid for shrublands and low tropical forests, and a 20 × 20 kilometer grid for arid ecosystems) is determined using INEGI's national land use and vegetation maps. The fact that all vegetation types (not just forests) are surveyed should benefit efforts to understand changes in atmospheric carbon as air passes over the continent [e.g., Denning *et al.*, 1999].

Mexican inventory plots are similar in design to national forest inventory plots used

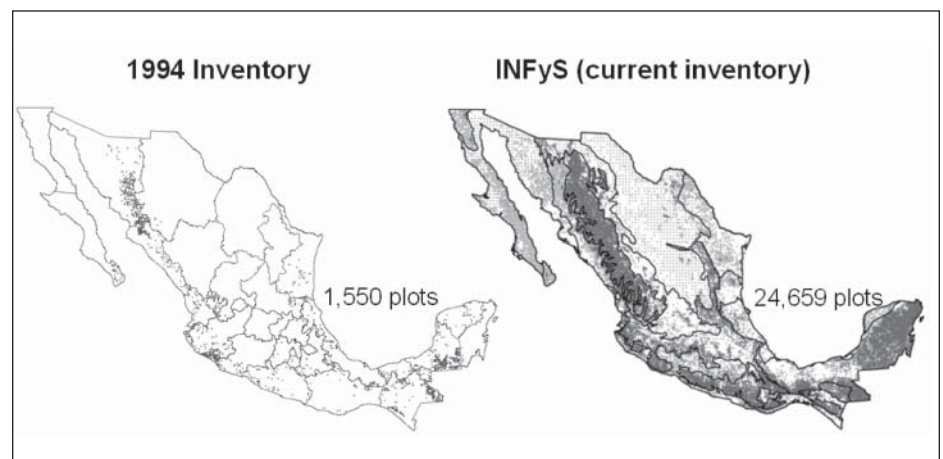


Fig. 1. Comparison of plot distributions supporting Inventario Nacional Forestal y de Suelos (INFyS) and the previous national forest inventory (1994 Inventario Nacional Forestal Periódico).